Anal. Chem. **2007,** *79,* 5711−5718

Steady-State Asymmetric Nanospray Dual Ion Source for Accurate Mass Determination within a Chromatographic Separation

Nicolas L. Young,*,†,‡ Michael C. Sisto,‡ Meggie N. Young,§ Patrick G. Grant,† David W. Killilea,# LaTasha LaMotte,‡ Kuang Jen J. Wu,† and Carlito B. Lebrilla‡

Biosecurity and NanoSciences Laboratory, Lawrence Livermore National Laboratory, Livermore, California 94551, Department of Chemistry, University of California, Davis, Davis, California 95616, College of Medecine, Drexel University, Philadelphia, Pennsylvania 19104, and Nutrition and Metabolism Center, Children's Hospital Oakland Research Institute, Oakland, California, 94609

Here we report the design, implementation, and initial use of an asymmetric steady-state continuous dual-nanospray ion source. This new source design consists of two independently controlled and continuously operating nanospray interfaces with funnel shaped counter electrodes. A steady-state ion mixing region combines the ions from the two sources into a single ion beam in the intermediate region after ion extraction from the nanospray sources but before the bulk of the pressure gradient of the vacuum interface. With this design we have achieved robust mixing of ions with no loss of duty cycle and remarkable ionization characteristics that appear entirely noncompetitive and potentially beneficial. This allows continuous introduction of internal mass calibration ions during a liquid chromatography−mass spectrometric analysis. This in turn allows for recalibration of individual spectra yielding sub part per million mass accuracy throughout the run. The steady-state approach presented here has several advantages over previous approaches. Since neither the voltage nor positions of the sprayers are changed, the nanospray has greater spray stability. The ions produced by the analyte sprayer are continuously sampled, as opposed to time-sharing which necessitates that the analyte ion stream be interrupted for some part of the duty cycle. There are no moving parts, no rapid changes to high voltages requiring additional control electronics, and no need for completely separate vacuum interfaces and the associated complexity. The sprayers are independently controlled and do not exhibit competition or mutual ionization suppression. This novel source has been implemented with a Bruker Apex II 9.4 T FTICR with a modified Apollo electrospray ion source as part of a nanoflow liquid chromatography−Fourier transform ion cyclotron resonance mass spectrometry analysis platform. Because of the low cost of implementation, the new source could potentially be applied to other forms of mass spectrometry, such as electrospray ionization-time-of-flight (ESI-TOF), which can benefit from internal mass calibration.

* Corresponding author. E-mail: young78@llnl.gov.
† Lawrence Livermore National Laboratory.
‡ University of California, Davis.
§ Drexel University.
# Children's Hospital Oakland Research Institute.

Fourier transform ion cyclotron resonance mass spectrometry (FTICR-MS) has very high mass resolution and potentially very high mass accuracy. The accuracy, however, is diminished by uncontrolled experimental parameters, often caused by variations in the ion population in the Penning trap producing variable space charge effects thus perturbing the resonant frequencies of the ions.[1,2] Several approaches have been taken to reduce the effect this has on the mass accuracy. It is possible to account for much of the frequency shift caused by varying ion populations by dynamically changing the calibration equation based on integrated signal intensity.[3] A different approach has been to control the number of ions in the trap either by selectively ejecting high abundance ions[4] or by varying the accumulation time based on an initial survey of the number of ions being introduced by the source.[5,6] These techniques provide significantly improved mass accuracy especially when well implemented. Another approach has been to introduce an internal mass calibrant (IMC) to allow for recalibration of each spectrum, thereby accounting for frequency shifts due to changing ion populations. With a simple infusion analysis, an IMC can be spiked into the sample, although this results in some ionization suppression. Dual sprayers for internal mass calibration are necessary when used in conjunction with chromatography because the standards are retained on and then eluted from the column, only being present at discrete retention times. An additional option is to introduce a postcolumn tee to introduce the IMC into the eluent flow; however, this dilutes the sample and broadens the peaks due to increased dead volumes and junctions, as well as creates significant ionization suppression.

It is possible to decouple the chromatographic separations from the mass spectrometric analysis such as by depositing the eluent

(1) Jeffries, J. B.; Barlow, S. E.; Dunn, G. H. *Int. J. Mass Spectrom. Ion Processes* **1983**, *54*, 169−187.
(2) Zhang, L.-K.; Rempel, D.; Pramanik, B. N.; Gross, M. L. *Mass Spectrom. Rev.* **2005**, *24*, 286−309.
(3) Easterling, M. L.; Mize, T. H.; Amster, I. J. *Anal. Chem.* **1999**, *71*, 624−632.
(4) Belov, M. E.; Anderson, G. A.; Angell, N. H.; Shen, Y.; Tolic, N.; Udseth, H. R.; Smith, R. D. *Anal. Chem.* **2001**, *73*, 5052−5060.
(5) Schwartz, J. C.; Zhou, X. G.; Bier, M. E. Method and Apparatus of Increasing Dynamic Range and Sensitivity of a Mass Spectrometer. U.S. Patent 5,572,-022, 1996.
(6) Page, J. S.; Bogdanov, B.; Vilkov, A. N.; Prior, D. C.; Buschbach, M. A.; Tang, K.; Smith, R. D. *J. Am. Soc. Mass Spectrom.* **2005**, *16*, 244−253.

10.1021/ac070446z CCC: $37.00
Published on Web 07/06/2007

onto a MALDI plate for subsequent analysis. Internal mass calibration can then be achieved by the InCAS method.[7] This approach can be automated such that it is an effective platform for analysis.[8] As an additional advantage, these approaches allow for random access querying of the LC trace but are in many ways complementary to on-line LC−ESI-MS approaches, and part of the motivation for their development was to circumvent the difficulty of introducing internal mass calibrant ions with electrospray systems.

Some previous implementations of dual spray technologies for the introduction of internal mass calibrant ions have used either mechanical[9−11] or electrical[12] control to alternate which ion plume is being sampled by the mass spectrometer. The ion plumes from two neighboring nanospray tips tend to repel each other due to Coulombic repulsion and resist mixing due to fluid dynamics. With a change in the position or potential on a sprayer, its associated spray plume may be made to dominate the sampling orifice of the mass spectrometer; however, it is difficult to reach a stable state where the plumes are both sampled by the mass spectrometer, much less have fine control over the ratio between the two. For this reason, previous implementations of dual spray sources have had to adjust the ratio of the plumes sampled by adjusting the amount of time of each duty cycle that each sprayer dominates the sampling orifice. This has been achieved by several ingenious methods with great impact on the ability to routinely achieve accurate masses during a chromatographic run and have consequently enabled significant advancements in the areas of science to which these approaches have been applied. Inherent in these approaches, however, are increased cost, complexity, and some loss of the duty cycle to the introduction of the IMC ions.

In order to circumvent the problems inherent in adjusting ion plume sampling rates with time, others have mixed the ion streams either before ion sampling or after the vacuum interface. Herniman et al. simply used two electrospray needles simultaneously in an otherwise unmodified ion source; however, this approach does not work with nanospray due to the lack of nebulization gases and associated turbulence to effectively mix the ion plumes.[13] Belov et al. constructed two parallel vacuum interfaces and a specially designed ion funnel to mix the ions after two separate vacuum interfaces.[14] The use of a "Y-tube" has previously been used to study ion−ion reactions between oppositely charged ions[15] but not previously considered suitable for the introduction of IMC.

In the present design, we demonstrate stable, robust, and adjustable mixing of ions from two sprayers in a continuous steady-state mode. The analyte or primary sprayer source and the subsequent ion path of the analyte ions are in an on-axis configuration, while the smaller vacuum interface capillary from the IMC sprayer source intersects and terminates into the main capillary at an acute angle about a centimeter after the main source. By separating the sprayers into two separate environments, we eliminate dueling sprayer plumes and can adjust the position of the sprayer to maximize ionization efficiency. These ion streams are mixed after the sampling orifices but before the bulk of the vacuum interface. In this region the ions are still entrained in significant amounts of bath gas that is being rapidly pulled into the mass spectrometer. The combination of the two streams under turbulent conditions likely allows the ion streams to effectively mix. The ratio between the two streams may be adjusted in two ways. The concentration of the mass calibration standard may be adjusted to adjust the concentration of the IMC ion plume. However, the better approach is to adjust the sampling rate of the IMC ion plume by reducing the sampling orifice and associated capillary diameter as in the present design. This results in more gas flow from the analyte ion source. Thus, by controlling steady-state fluid mixing, the desired ratio of sampling rates between the sources previously controlled by time or post source ion optics can be achieved.

To demonstrate the utility of this design, we analyzed the mass accuracy and source characteristics in continuous infusion mode where conditions can be held constant. We also demonstrate its use in combination with nanoflow liquid chromatography separations. We found this design to exhibit exceptional ionization suppression effects that appear minimal and in some cases even beneficial.

EXPERIMENTAL SECTION

Materials. Human angiotensin I, bovine albumin, equine alcohol dehydrogenase, porcine alpha amylase, bovine carbonic anhydrase, bovine catalase, mollusk hemocyanin, bovine hemoglobin, bovine holo-transferrin, jack bean type III urease, and bovine xanthine oxidase were purchased from Sigma Aldrich (St. Louis, MO). Agilent ES Tune Mix was purchased from Agilent Technologies (Palo Alto, CA). HPLC grade acetonitrile was purchased from Honeywell Burdick and Jackson (Morristown, NJ). Pure water (18 MΩ cm) was used throughout.

Column and Nanospray Tip Manufacture. The nanospray tips were produced in-house from 75 μm internal diameter (i.d.) fused silica tubing using a Sutter Instruments Co. model P2000 laser tip puller. The chromatographic stationary phase of 5 μm Luna C18 (Phenomenex, Torrance, CA) was packed directly into the nanospray tip by bomb loading a slurry in 70% ethanol such that the nanospray tip and the chromatographic column are integrated with the column terminating at the approximately 15 μm diameter nanospray tip.

NanoLC—FTICR-MS Instrumentation. The nanoliquid chromatography pumps used in this work were a prototype nanoLC pump developed by Eksigent Technologies (Dublin, CA) used for the internal mass calibration standard channel and a 2D-nanoLC system also by Eksigent Technologies (Dublin, CA).

The mass spectrometer is a 9.4 T Apex II Fourier transform ion cyclotron resonance mass spectrometer (Bruker Daltonics, Billerica, MA) with a modified Apollo source. Part of the Apollo source is used in the new nanospray source design. Aside from

(7) O'Connor, P. B.; Costello, C. E. *Anal. Chem.* **2000**, *72*, 5881−5885.
(8) Brock, A.; Horn, D. M.; Peters, E. C.; Shaw, C. M.; Ericson, C.; Phung, Q. T.; Salomon, A. R. *Anal. Chem.* **2003**, *75*, 3419−3428.
(9) Hannis, J. C.; Muddiman, D. C. *J. Am. Soc. Mass Spectrom.* **2000**, *11*, 876−883.
(10) Nepomuceno, A. I.; Muddiman, D. C.; Bergen, H. R.; Craighead, J. R.; Burke, M. J.; Caskey, P. E.; Allan, J. A. *Anal. Chem.* **2003**, *75*, 3411−3418.
(11) Wolff, J. C.; Eckers, C.; Sage, A. B.; Giles, K.; Bateman, R. *Anal. Chem.* **2001**, *73*, 2605−2612.
(12) Satomi, Y.; Kudo, Y.; Sasaki, K.; Hase, T.; Takao, T. *Rapid Commun. Mass Spectrom.* **2005**, *19*, 540−546.
(13) Herniman, J. M.; Bristow, T. W. T.; O'Connor, G.; Jarvis, J.; Langley, G. J. *Rapid Commun. Mass Spectrom.* **2004**, *18*, 3035−3040.
(14) Belov, M. E.; Zhang, R.; Strittmatter, E. F.; Prior, D. C.; Tang, K.; Smith, R. D. *Anal. Chem.* **2003**, *75*, 4195−4205.
(15) Ogorzalek Loo, R. R.; Udseth, H. R.; Smith, R. D. *J. Am. Soc. Mass Spectrom.* **1992**, *3*, 695−705.

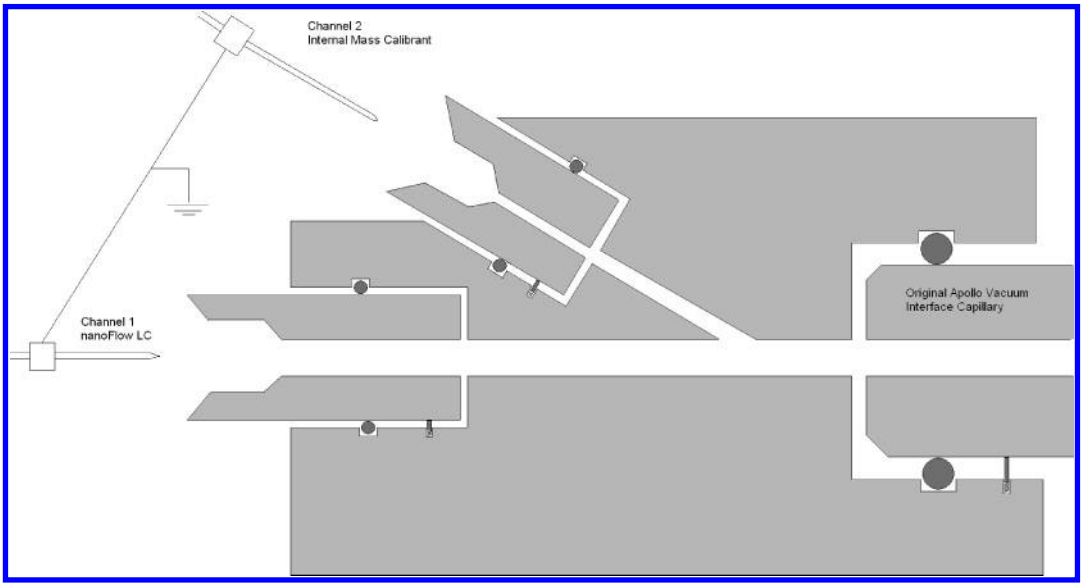

Figure 1. Schematic diagram of the new steady-state dual spray ion source (not drawn to scale). The spray tips are grounded and the counter electrodes are held at approximately −2000 V. Electrical contact is made between all metal parts spring loaded contacts, and all junctions are made airtight by plastic o-rings.

the specific design changes to allow steady-state dual spray, the drying gas heater has been modified to deliver drying gas temperatures up to about 400 °C and is operated at 350 °C here. The main purpose of this gas is to heat the glass capillary which serves as the vacuum interface to the mass spectrometer.

Source Description. As can be seen in Figure 1, in this novel nanospray interface two pulled glass capillaries are kept at ground potential through liquid junctions of platinum wire with the solvent in a low dead-volume tee. The nanospray potential of approximately −2 kV is delivered to the counter electrodes/sampling orifices of the mass spectrometer. On the original Apollo electrospray source, the sampling orifice was on a flat surface and was approximately 0.5 mm in diameter. Instead, each of the new sources sees an approximately 3 mm entrance that is later reduced to 0.5 or 0.2 mm. The primary potential that the nanospray tip sees is from an inverted cone that extends from the 3 mm orifice at a slightly obtuse angle. The nanospray tips are placed on-axis with respect to each inverted cone approximately 1 cm from the 0.5 or 0.2 mm orifice. The effect of this geometry is that the ions are forced to traverse a distance of approximately 1 cm of atmospheric pressure, effectively desolvating the ions, yet are also effectively entrained in directed fluid dynamic flows into the mass spectrometer. Additionally, the electrostatics of the geometry enforce the boundary conditions of Taylor cone formation.[16] This geometry has been previously employed by us for a single sprayer with good results and has been shown by others to improve sensitivity by as much as 3-fold with both electrospray and AP-MALDI sources.[17−19]

Each counter electrode/sampling orifice is a removable stainless steel insert that mates with and makes electrical connection by a spring loaded contact to a stainless steel union piece that in turn mates with the standard metal coated glass vacuum transfer capillary of the Bruker Daltonics Apollo ion source. In the current configuration, the second port insert is smaller than the primary port insert. The primary ion source and all subsequent ion transfer mechanisms (primary ion channel) are directly on-axis with a direct line of sight to the ICR cell. The secondary ion source through which the IMC ions are introduced (secondary ion channel) is placed at an acute angle of about 30° off-axis, and the smaller ion transfer capillary intersects the primary ion channel in the junction piece before the standard ion transfer capillary.

Accurate Mass Determination. To confirm the well-established capability to achieve sub ppm mass accuracy with the use of internal mass calibration standards with this particular source design, angiotensin was infused on the primary channel while the internal mass calibration standard was infused in the secondary channel. Each experiment consisted of 8 coadded acquisitions, and 100 experiments were performed in series.

Infusion Characterization of the Source. In order to best characterize the fundamentals of this novel source design in regards to behavior and performance, several infusion studies were performed. For each study, each spectrum consisted of the sum of eight transients and five replicate spectra were performed for each condition per experiment unless otherwise stated.

In order to characterize how the second ion stream affects the primary ion stream, a large loop injection of 1 pmol/μL angiotensin I in 50% acetonitrile and 0.1% formic acid was introduced to the stream leading to the primary nanospray tip. After the signal was observed and stabilized, five sets of spectra were acquired. During the same loop injection, the internal standard was introduced into the second channel and an identical set of five spectra were acquired. This was repeated five times under different ionization conditions, on different days, and with the internal standard and no internal standard data acquired in random order. Two additional data sets were acquired with a lower mass range to characterize the role of the third charge state of angiotensin.

(16) Taylor, G. *Proc. R. Soc. London, Ser. A* **1964**, *280*, 383−397.
(17) Lee, S.; Young, N. L.; Whetstone, P. A.; Cheal, S. M.; Benner, W. H.; Lebrilla, C. B.; Meares, C. F. *J. Proteome Res.* **2006**, *5*, 539−547.
(18) Wu, S.; Zhang, K.; Kaiser, N. K.; Bruce, J. E.; Prior, D. C.; Anderson, G. A. *J. Am. Soc. Mass Spectrom.* **2006**, *17*, 772−779.
(19) Prior, D. C.; Price, J.; Bruce, J. E. Sample Inlet Tube for Ion Source. U.S. Patent 6,455,846, 2002.

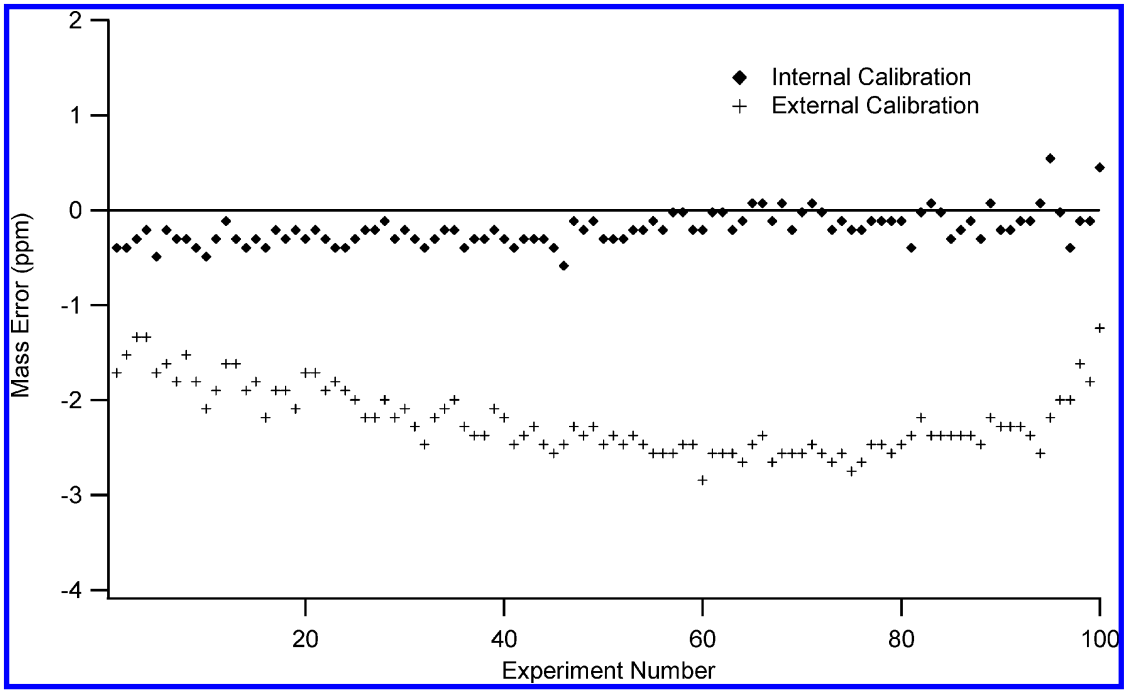

Figure 2. Comparison of internal versus external calibration of the [M + 2H] peak of angiotensin I. The two data series are the same data and only differ by calibration procedure. The internally calibrated data was calibrated for each spectrum based on the IMC masses. The externally calibrated data was calibrated once directly before acquisition.

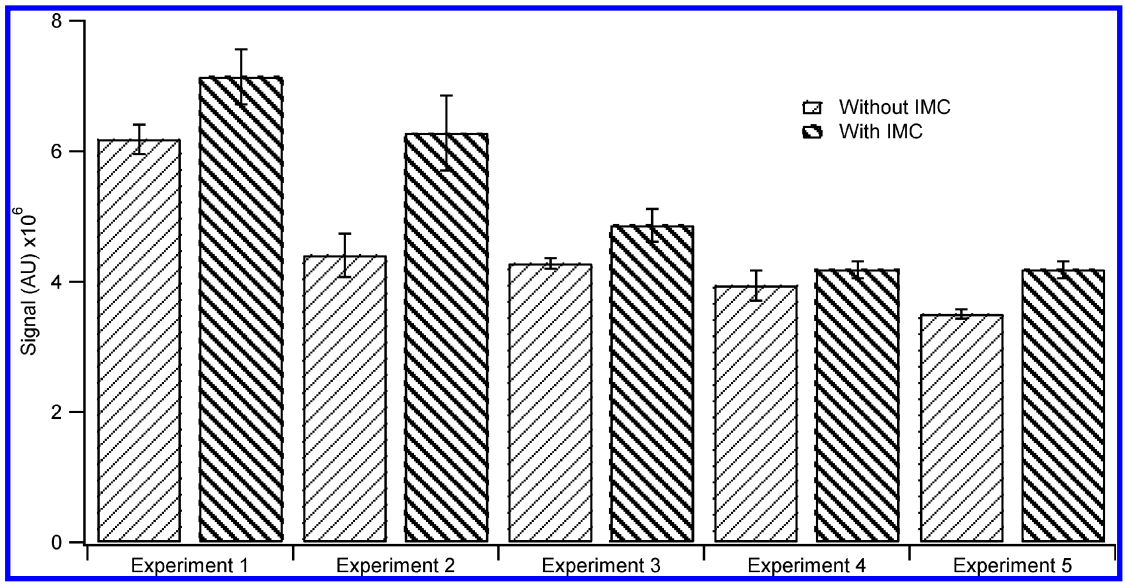

Figure 3. Comparison of signal intensity of the [M + 2H] ion of angiotensin I at 648 *m*/*z* with and without the IMC channel active. In all cases, the ion signal is stronger with the IMC channel active. In experiments 1, 3, and 4 the "without IMC" experiment was performed first. In experiments 2 and 5 the "with IMC" experiment was performed first. Experiments 4 and 5 share the same "with IMC" data and are coupled. Experiment 1 was performed a day earlier than the other experiments, and the tuning parameters were varied between experiments (except between experiments 4 and 5). Error bars are 1 standard deviation.

A similar experiment was performed using substance P, also at 1 pmol/μL, as the analyte to confirm the angiotensin results. In this experiment, 64 spectra were coadded for each spectrum and a total of six experiments were performed. One replicate was acquired per condition in each experiment. The condition with the IMC channel active was always acquired first. This experiment is designed to take advantage of signal averaging to reduce variations due to signal instability at the cost of reduced error statistics.

The effect of the first channel on the second channel was characterized by removing the angiotensin being sprayed by the primary sprayer and observing the effect on the internal standard signal at 622 *m*/*z*.

The effect of the second port on the primary channel due to fluid dynamics caused by the introduction of air was characterized by physically blocking the second channel. Spectra were acquired as above with and without the second port blocked but with the nanospray tip absent.

NanoLC—FTICR Analysis. A sample containing an approximately equal mass mixture of 10 proteins was prepared giving a mixture of unequal molar abundance. All proteins were purchased directly from commercial manufacturers. The sample was

Table 1. The Effects of the Internal Mass Calibrant (IMC) Channel on the Intensity of 1 pmol/μL Substance P in 50% Acetonitrile, 0.1% Formic Acid[a]

experiment number	analyte (Substance P) ion signal $\times 10^7$ (IMC channel inactive)	analyte (Substance P) ion signal $\times 10^7$ (IMC channel active)
1	1.6	1.7
2	1.3	1.2
3	1.1	1.1
4	1.1	0.9
5	1.6	1.7
6	1.2	1.4
average	1.32	1.33

[a] 64 spectra were coadded for each experiment, and all six experiments used identical conditions. The IMC is undiluted Agilent tune mix. The condition with the IMC channel active (right column) was always acquired first.

digested for 4 h with mass spectrometry grade trypsin gold (Promega Corporation, Madison, WI) using recommended digestion conditions and zip tip purification procedures. The sample was loaded onto the 75 μm internal diameter by 20 cm column and eluted by a 200 nL/min gradient from 5% to 55% B in 40 min (A, 0.1% formic acid; B, 90% acetonitrile/0.1% formic acid). Four 512k acquisitions were coadded every 12 s without quenching the hexapole ion trap between ion injections.

RESULTS AND DISCUSSION

Accurate Mass Validation. The new source design provides the capability of determining masses of analyte ions to within 1 ppm mass accuracy. When angiotensin was infused on the primary channel while the IMC (Agilent ES Tune Mix, a mixture of fluorophosphazines) was infused in the secondary channel. All analyte masses were within 0.6 ppm mass accuracy (0.8 mDa) after internal recalibration as shown in Figure 2. These 100 data points reflect an rms error of 0.26 ppm (0.34 mDa) with a mean error of −0.20 ppm (0.26 mDa), and the rms deviation from the mean error is 0.17 ppm (0.22 mDa). The standard deviation from the actual mass value is 0.26 ppm (0.34 mDa), and this indicates a reasonable maximum mass deviation (MMD) of 3σ to be 0.78 ppm (1 mDa). The externally calibrated data was calibrated once directly before acquisition.

The externally calibrated data exhibits drift of 1.6 ppm (2.1 mDa) and a systematic error of 2.2 ppm (2.8 mDa). Note that this represents a best effort to achieve good external calibration by calibrating minutes before beginning the experiment and maintaining continuous infusion of both analyte (channel 1) and IMC (channel 2) to deliver an approximately constant ion population. The use of IMCs to achieve such mass accuracies is well-established; however, we can conclude that our method works to achieve such accuracies within a nanoLC−FTICR analysis with substantially less effort and cost than other methods.

Ion Source Behavior. The ion source exhibits exceptionally little suppression of the analyte signal, and in some cases an increase in analyte signal is observed. Such an increase in analyte signal strength was observed for angiotensin. Under all conditions tried, the introduction of the IMC in the second ion stream consistently had a statistically significant positive effect on the ion signal of the doubly charged angiotensin ion at 648 *m/z*. The 5 data sets consist of 10 spectra each, 5 with and 5 without the second ion stream of internal mass calibration standards present. The results for each of these data sets are summarized in Figure 3.

All five experiments exhibited an increase in signal when the IMC channel was active with percent increases of 16%, 43%, 14%,

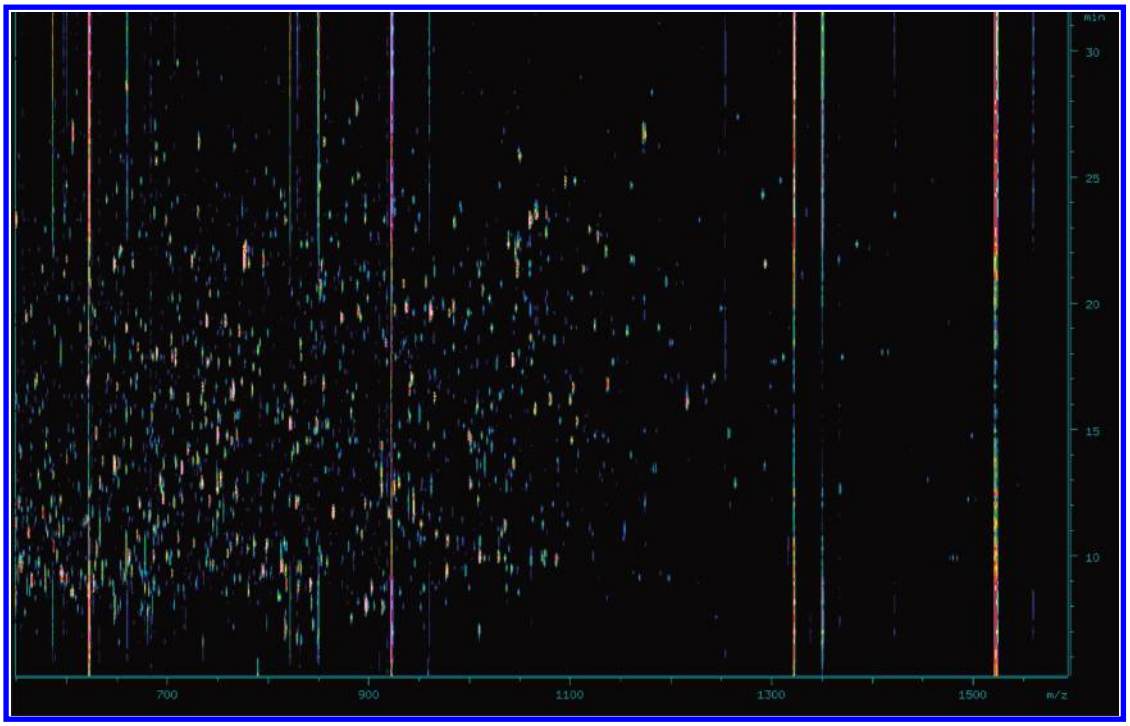

Figure 4. LC−MS contour map of the nanoLC−FTICR analysis of a tryptic digest of a mixture of 10 proteins. Note that the masses at 622, 922, and 1522 *m*/*z* are present continually as they are introduced into the mass spectrometer from the secondary ion channel in infusion mode while the tryptic peptides are eluting from the column to the primary ion source.

Table 2. Peptides Corresponding to Bovine Holo-Transferrin Identified from the NanoLC–FTICR Analysis[a]

amino acid sequence	theoretical MW	observed MW internal calibration	error (ppm) internal calibration	observed MW external calibration	error (ppm) external calibration
AISNNEADAVTLDGGLVYEAGLK	2320.1673	2320.1677	0.19	2320.1633	−1.70
DNPQTHYYAVAVVK	1604.8073	1604.8063	−0.61	1604.8035	−2.36
DTDFKLNELR	1250.6381	1250.6373	−0.64	1250.6355	−2.07
DTDFKLNELR	1250.6381	1250.6377	−0.32	1250.636	−1.68
LYKELPDPQESIQR	1715.8968	1715.8978	0.57	1715.8958	−0.60
LYKELPDPQESIQR	1715.8968	1715.8961	−0.43	1715.894	−1.65
ELPDPQESIQR	1311.6545	1311.6553	0.63	1311.6527	−1.35
ELPDPQESIQR	1311.6545	1311.6545	0.02	1311.6527	−1.35
HSTVFDNLPNPEDR	1640.7669	1640.7654	−0.90	1640.762	−2.97
HSTVFDNLPNPEDR	1640.7669	1640.7683	0.87	1640.7626	−2.61
HSTVFDNLPNPEDRK	1768.8618	1768.8611	−0.42	1768.8601	−0.98
HSTVFDNLPNPEDRK	1768.8618	1768.8611	−0.42	1768.8593	−1.44
TVGGKEDVIWELLNHAQEHFGK	2507.2683	2507.2678	−0.20	2507.2644	−1.56
DKPDNFQLFQSPHGK	1757.8611	1757.8601	−0.58	1757.8577	−1.94
DKPDNFQLFQSPHGK	1757.8611	1757.8602	−0.52	1757.8583	−1.60
DLLFK	635.3768	635.3764	−0.69	635.3754	−2.26
DLLFKDSADGFLK	1468.7688	1468.7678	−0.66	1468.7649	−2.64
DLLFKDSADGFLK	1468.7688	1468.7679	−0.60	1468.765	−2.57
DSADGFLK	852.4103	852.4107	0.44	852.4083	−2.38
DSADGFLK	852.4103	852.4102	−0.15	852.4086	−2.02
DSADGFLK	852.4103	852.4108	0.56	852.4083	−2.38
DSADGFLKIPSK	1277.6741	1277.6747	0.43	1277.6726	−1.21
ESKPPDSSK	974.4795	974.4786	−0.89	974.4761	−3.45
IMKGEADAMSLDGGYLYIAGK	2203.0779	2203.0759	−0.91	2203.0732	−2.14
IMKGEADAMSLDGGYLYIAGK	2203.0779	2203.0767	−0.55	2203.0723	−2.55
GEADAMSLDGGYLYIAGK	1830.8584	1830.8578	−0.33	1830.8512	−3.93
GEADAMSLDGGYLYIAGK	1830.8584	1830.8578	−0.33	1830.8507	−4.21
CGLVPVLAENYK	1305.6877	1305.6882	0.39	1305.6887	0.78
NTPEKGYLAVAVVK	1488.8426	1488.8422	−0.27	1488.8401	−1.68
NTPEKGYLAVAVVK	1488.8426	1488.843	0.26	1488.8397	−1.95
TSDANINWNNLK	1389.6763	1389.6764	0.09	1389.6726	−2.64
TSDANINWNNLKDK	1632.7982	1632.798	−0.11	1632.7942	−2.44
TSDANINWNNLKDK	1632.7982	1632.7969	−0.78	1632.7939	−2.62
TAGWNIPMGLLYSK	1550.8041	1550.8051	0.64	1550.8022	−1.23
TAGWNIPMGLLYSK	1550.8041	1550.8027	−0.91	1550.8018	−1.49
TAGWNIPMGLLYSK	1550.8041	1550.8029	−0.78	1550.8019	−1.43
TAGWNIPMGLLYSK	1550.8041	1550.804	−0.07	1550.8024	−1.11
TAGWNIPMGLLYSK	1550.8041	1550.8044	0.18	1550.8027	−0.91
GDVAFVK	735.4041	735.4039	−0.30	735.3975	−8.96
GDVAFVKDQTVIQNTDGNNNEAWAK	2734.3073	2734.3091	0.67	2734.2983	−3.28
GDVAFVKDQTVIQNTDGNNNEAWAK	2734.3073	2734.3083	0.38	2734.2991	−2.99
GDVAFVKDQTVIQNTDGNNNEAWAK	2734.3073	2734.3057	−0.57	2734.2993	−2.92
GDVAFVKDQTVIQNTDGNNNEAWAK	2734.3073	2734.3076	0.12	2734.2982	−3.30
GDVAFVKDQTVIQNTDGNNNEAWAK	2734.3073	2734.3098	0.92	2734.301	−2.29
DQTVIQNTDGNNNEAWAK	2017.9215	2017.9205	−0.52	2017.9125	−4.48
DQTVIQNTDGNNNEAWAK	2017.9215	2017.9233	0.87	2017.9178	−1.86
ATCVEKILNK	1118.6244	1118.625	0.57	1118.6233	−0.95
ILNKQQDDFGK	1305.6803	1305.6793	−0.76	1305.6791	−0.91
ILNKQQDDFGK	1305.6803	1305.6794	−0.68	1305.6801	−0.15
ILNKQQDDFGK	1305.6803	1305.6797	−0.45	1305.6819	1.23
ILNKQQDDFGK	1305.6803	1305.6801	−0.15	1305.6829	2.00
ILNKQQDDFGK	1305.6803	1305.6794	−0.68	1305.6823	1.54
DLLFR	663.3830	663.3825	−0.73	663.381	−3.00
DLLFRDDTK	1122.5795	1122.5797	0.16	1122.5784	−1.00
KTYDSYLGDDYVR	1594.7389	1594.7393	0.23	1594.7367	−1.40
KTYDSYLGDDYVR	1594.7389	1594.7391	0.10	1594.7358	−1.96
KTYDSYLGDDYVR	1594.7389	1594.739	0.04	1594.7349	−2.53
TYDSYLGDDYVR	1466.6440	1466.6428	−0.80	1466.6407	−2.23
TYDSYLGDDYVR	1466.6440	1466.6429	−0.73	1466.6396	−2.98

[a]Multiple entries for a given peptide represent consecutive spectra as the peptide eluted. The external calibration is based on one spectrum at the beginning of the run.

6%, and 19%. These data were collected under varying experimental conditions, and within each experiment the order of conditions were randomized. Overall, the average of these data sets corresponds to an average increase of 19% with a standard deviation of 14% which corresponds to a 90% confidence interval of 20%. Nanospray is by nature not particularly reproducible or quantitative, yet this data seems to indicate a modest enhancement in signal intensity of the angiotensin introduced from the primary channel when the IMC is infused on the secondary channel.

In an effort to explain this phenomenon, the mass range was expanded to lower masses to observe the relationship of the signal intensity of the third charge state of angiotensin to the second

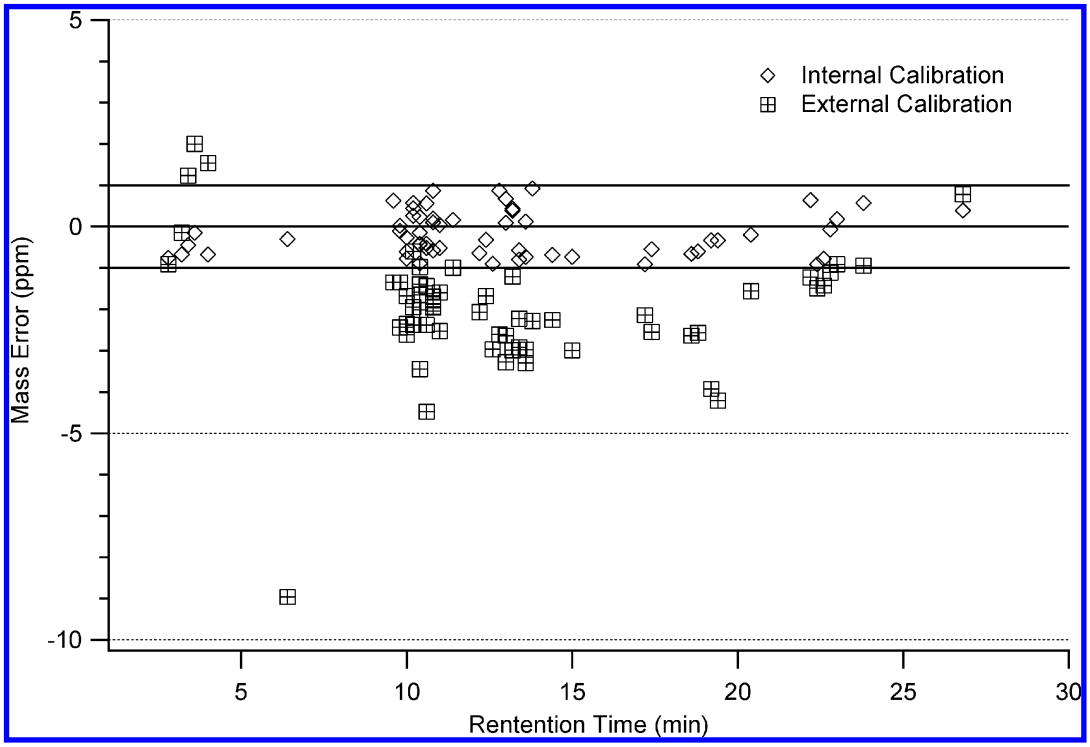

Figure 5. A comparison of internally versus externally calibrated data from the nanoLC−FTICR analysis of a trypsin digestion of a nonequimolar mixture of 10 proteins. The data are the same, only the calibration procedure used differs. The externally calibrated data is calibrated once at the beginning of data acquisition. This is significantly better external calibration than the usual practice of calibrating hours or days before hand, yet significant errors are observed.

charge state under the two conditions. While we observed similar increases in the signal strength of the 648 m/z ion of 20% and 18% in the two datasets acquired, we did not observe a statistically significant change in the 433 m/z signal of 6% and −4%, and there was a net increase in total angiotensin signal of 13% and 6% for the two experiments. This indicates that the signal increase is likely not due to a process that converts the ions between charge states such as charge stripping. The apparent increase in signal from this process may be due to gas-phase proton-transfer reactions that occur during or after the mixing process and may be dependent on the choice of IMC. Although any increase in signal is likely system specific, this would allow for the selection of IMCs that could further enhance the analyte signal. At the least, these results demonstrate that this new source design does not generally result in significant loss to the analyte signal.

The two ion sources appear completely independent, and the mixing of the two ion streams between the ion sources and the bulk of the vacuum interface appears robust, reproducible, and noncompetitive. When similar experiments were run using substance P as the analyte, a less significant increase was observed as summarized in Table 1. This data also averaged more signal per data point, and therefore should be less prone to short term noise; however, long-term drift is not improved by this approach. The slight increase observed in this experiment is not statistically significant. It does however demonstrate that there is no significant decrease in signal either. The analyte signal (substance P) is essentially unaffected by changing from a condition where it is the sole dominant signal in the spectrum (when the IMC channel is off) to a condition where there are multiple calibrant ions of equal or greater absolute intensity (when the IMC channel is on). This demonstrates a remarkable lack of ionization suppression or channel cross-talk.

When the secondary port was blocked such that air could not flow into the port, there was no significant change in ion signal (−1%) relative to the port being unobstructed but without an ion stream. This indicates that the flow of bath gas into the secondary port does not affect the primary ion stream significantly either positively or negatively.

The results did not indicate any effect from the first ion stream on the secondary stream with less than 0.5% change in both of two repeated experiments averaging five relatively unstable spectra for each condition and each data set. This was not investigated further since the effect is inconsequential.

NanoLC—FTICR Analysis. The LC−MS data from the nanoLC−FTICR anaylsis of the tryptic digest of 10 proteins in a nonequimolar mixture is shown in the contour map in Figure 4. The proteins used were bovine albumin, equine alcohol dehydogenase, porcine alpha amylase, bovine carbonic anhydrase, bovine catalase, mollusk hemocyanin, bovine hemoglobin, bovine holotransferrin, jack bean type III urease, and bovine xanthine oxidase. The internal standard peaks are persistent while the peptides elute from the column. Nine out of ten proteins were detected, with the largest and therefore least abundant protein missing. Table 2 lists the peptides and associated mass errors for bovine holotransferrin. Note that when multiple sequential spectra detect the same peptide as it elutes from the column, the externally calibrated mass error often varies significantly from spectrum to spectrum. When the same peptides identified with internal mass calibration are measured using a single spectrum for calibration at the beginning of the run (external calibration), the error increases

with most ions outside of the 1 ppm error bars and a saddle-shaped trend throughout the run can be seen as shown in Figure 5. This trend is a result of increased ion populations in the ICR cell as more ions elute in the middle of the run. Thus we have successfully implemented this new source design in our nanoLC−FTICR analysis platform to achieve the benefit of high mass accuracy provided by internal mass calibration while maintaining the greater dynamic range, sensitivity, and specificity afforded by high-resolution chromatography.

CONCLUSIONS

A new dual spray nanospray ion source which represents a significant improvement in cost, robustness, and reliability has been demonstrated to not only provide sub part per million mass accuracy during chromatographic analyses but at a cost to analyte signal that is either low or possibly even beneficial under certain conditions. This technology can easily be extended to all electrospray based mass spectrometers such as high-resolution electrospray-TOFs and Orbitrap instruments, where it will have the most utility, given little cost both monetarily and analytically, but also to quadrupole and ion trap mass spectrometers. With a simple yet thoughtfully designed interface, two ion streams have been introduced to a mass spectrometer simultaneously in a steady-state fashion with essentially one vacuum interface in a manner that preserves the ion signal of the primary analyte channel. The difference between this design and previous designs in terms of monetary cost, complexity, and ease of implementation is exceptional. Many previous designs also fundamentally came with a cost to analytical metrics, such as decreased sensitivity, which for many applications made implementation not worthwhile. With orders of magnitude less monetary cost and no negative impact on analyte signal, this source makes possible the ubiquitous use of internal mass calibrants in mass spectrometry where previously the cost to benefit ratio inhibited it.

ACKNOWLEDGMENT

This work was supported by the Department of Energy Advanced Study Program to N.L.Y., NIH Grant GM049077 to C.B.L., and NIH Grant GM074819-02 to P.G.G. and D.W.K. The authors would like to thank Dr. Gary H. Kruppa for providing portions of the data analysis software and software development assistance. Portions of this work were performed under the auspices of the U.S. Department of Energy by University of California, Lawrence Livermore National Laboratory under Contract W-7405-Eng-48.

Received for review March 5, 2007. Accepted May 25, 2007.

AC070446Z